Activity of and Initial Mechanistic Studies on a Novel Antileishmanial Agent Identified through in Silico Pharmacophore Development and Database Searching

Dawn A. Delfín,[†] Apurba K. Bhattacharjee,[‡] Adam J. Yakovich,[†] and Karl A. Werbovetz*,[†]

Division of Medicinal Chemistry and Pharmacognosy, College of Pharmacy, The Ohio State University, Parks Hall Room 331, 500 West 12th Avenue, Columbus, Ohio 43210, and Division of Experimental Therapeutics, Walter Reed Army Institute of Research, 503 Robert Grant Avenue, Silver Spring, Maryland 20901

Received February 10, 2006

A 3D pharmacophore was generated to describe the antileishmanial activity of dinitroaniline sulfonamides by CATALYST 3D-QSAR methodology, and this pharmacophore was used to search the Maybridge database. Two compounds identified in this search, BTB 06237 and BTB 06256, were highly active with IC_{50} values against *L. donovani* amastigotes of 0.5 ± 0.2 and 2.3 ± 0.8 μM, respectively. BTB 06237 also reduced parasite burdens in *L. mexicana*-infected J774 macrophages at low micromolar concentrations. Unlike the dinitroaniline sulfonamides, the active compounds did not display antimitotic effects against *Leishmania*. Transmission electron microscopy showed that the single parasite mitochondrion becomes dilated following incubation with BTB 06237, and fluorescence microscopy demonstrated that this organelle fragments into intensely staining spheres when treated with a mitochondrion-specific dye. The mitochondrial membrane potential was also dissipated in BTB 06237-treated parasites. These results indicate that BTB 06237 is an intriguing antileishmanial lead compound that likely interferes with mitochondrial function.

Introduction

Leishmaniasis, a disease caused by protozoan parasites of the genus *Leishmania*, currently afflicts 12 million people worldwide with 2 million new cases reported annually.[1] Without effective treatment, visceral leishmaniasis is associated with a near 100% fatality rate, whereas other forms can be severely debilitating.[2,3] Current treatments are not ideal because they possess one or more negative attributes, including toxicity, loss of effectiveness due to resistance, expense, and inconvenience.[4−7] Novel therapies to combat leishmaniasis are urgently needed.

We have previously demonstrated the antileishmanial activity of several dinitroaniline sulfonamide compounds based on the herbicide oryzalin.[8−10] These compounds inhibit purified parasite tubulin polymerization and arrest parasite growth in the G_2/M phases of the cell cycle. Furthermore, the lead compounds in this series, **1** (N^1-phenyl-3,5-dinitro-N,$^4N^4$-di-*n*-propyl sulfanilamide, GB-II-5) and **11** (N^1-phenyl-3,5-dinitro-N,$^4N^4$-di-*n*-butyl sulfanilamide, GB-II-150, see Table 1 for structures), were more active against *L. donovani* parasites than mammalian cells and were selective for leishmanial tubulin over purified porcine brain tubulin.[9,10] The activity of these analogues were greatly improved over the activity of the original lead compound oryzalin.[8] Encouraged by these results, a quantitative structure−activity relationship study of these dinitroaniline sulfonamides was performed using CATALYST software (Accelrys, Inc.). A 3D pharmacophore was developed highlighting the antileishmanial features of the dinitroaniline sulfonamides and cross-validated against a test set. The pharmacophore's template was used to search the Maybridge compound database to identify novel agents with potential leishmanicidal activity. The most promising compounds identified through this search were selected and tested against *L. donovani*. We report the identification and evaluation of two highly active and five moderately active antileishmanial compounds using this methodology. We also report the studies investigating the cellular effects of the most active agent, BTB 06237 (**46**, see structure in Table 4), on *Leishmania* parasites.

Results

Molecular Modeling. CATALYST methodology was used to generate 60 distinct 3D pharmacophore models of the antileishmanial activity of 15 dinitroaniline sulfonamides (training set, Table 1). The most statistically significant pharmacophore contained an aliphatic hydrophobic group, an aromatic hydrophobic group, an additional aromatic functionality, and a hydrogen bond acceptor (Figure 1a). This pharmacophore was the best at estimating the activity of the compounds in the training set and showed a strong correlation between the estimated and experimental activities ($r^2 = 0.95$, Figure 2a). Furthermore, this pharmacophore was cross-validated by its ability to estimate the activities of 14 other dinitroaniline sulfonamides in a test set (Table 2), which also shows a strong correlation ($r^2 = 0.88$, Figure 2b). Outside of the 29 compounds in the training and test sets whose activities the pharmacophore was able to predict, there were an additional 9 compounds whose activities the pharmacophore was not able to predict (Table 3). Statistically, the pharmacophore shown in Figure 1a had a low chance of representing a true correlation between the structure and activity according to the bit score (the bit score represents the robustness of the correlation between pharmacophore predictive ability and experimental values). Despite this, the pharmacophore was remarkably successful in predicting the activities of the compounds in both the training and test sets and succeeded in identifying new compounds with antileishmanial activity as outlined below.

The pharmacophore template was used to search the 55 000 molecules in the Maybridge compound database. Two types of searches were performed: one with only the pharmacophore and the other with the most active dinitroaniline sulfonamide

* Corresponding author. Tel: (614) 292-5499. Fax: (614) 688-8556. E-mail: werbovetz.1@osu.edu.
[†] The Ohio State University.
[‡] Walter Reed Army Institute of Research.

10.1021/jm060156v CCC: $33.50
Published on Web 06/08/2006

Table 1. Structures of the Training Set Compounds with Their Experimental and CATALYST-Estimated IC_{50} Values against *L. donovani* Axenic Amastigotes[a]

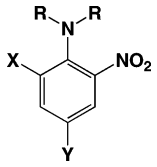

Compound	R	X	Y	Experimental IC_{50} (μM)	Estimated IC_{50} (μM)
oryzalin	n-propyl	NO_2	SO_2NH_2	65 ± 4^b	69
1	n-propyl	NO_2		5.0 ± 1.1^b	7.6
2	n-propyl	NO_2	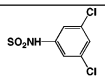	3.7 ± 0.9^b	1.6
3	n-propyl	NO_2	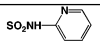	60 ± 6^b	49
4	n-propyl	NO_2	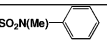	21 ± 3^b	17
5	n-propyl	NO_2	$SO_2N(CH_2CH_3)_2$	27 ± 0^b	46
6	n-propyl	NO_2	$SO_2NHCH_2CH_2CH_3$	54 ± 9^b	46
7	n-propyl	NO_2	$SO_2N(CH_2CH_2CH_3)_2$	55 ± 3^b	49
8	n-propyl	NO_2	$SO_2NH(CH_2)_3CH_3$	50 ± 24^b	52
9	n-propyl	NO_2		43 ± 2^b	63
10	n-propyl	NO_2		50 ± 7^b	59
11	n-butyl	NO_2		2.6 ± 0.3^b	5.4
12	n-butyl	NO_2	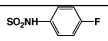	5.6 ± 0.2	5.7
13	n-propyl	NO_2	$C \equiv N$	$>100^c$	78
14	n-propyl	NO_2		$>100^c$	61

[a] The error is reported as the standard deviation from the mean of three separate experiments. [b] From ref 10. [c] From ref 8.

(compound **11**, see Table 1) mapped onto the pharmacophore (Figure 1b). The latter search permitted the consideration of the steric contribution of the compound with the other pharmacophoric features as part of the search criteria. Three hundred compounds (hits) were reported for each search. The pharmacophore assessed a fit score (quantification of the compounds' relative abilities to fit into the pharmacophore) for each of the hits and reported the conformational energy requirement of the best-fitting conformer. Both figures give a relative indication of the expected activity of these compounds. The fit scores of the hits ranged from less than 1 to 7.67, with **11** having a fit score of 7.47 in the pharmacophore. Only the best-fitting hits (fit score >4.5) for which the best-fitting conformer had low conformational energy costs (<15 kcal/mol) were retained for further analysis, leaving 125 compounds from the pharmacophore-only search and 78 compounds from the steric-pharmacophore search.

Antileishmanial Activities. The most promising of the remaining hits were selected for testing against *L. donovani* axenic amastigotes in vitro. These compounds had the best fit scores (≥6.0) and lowest conformational energies (∼10 kcal/mol or lower). The number of compounds tested was limited to 19 by the in-stock availability at Maybridge Organics. Compounds **46** (BTB 06237, see Table 4) and **48** (BTB 06256) displayed high antileishmanial activity with IC_{50} values of 0.5 ± 0.2 and 2.3 ± 0.8 μM, respectively. These compounds also showed selectivity because **46** and **48** inhibited the growth of Vero cells (African Green Monkey cells) at higher concentrations (IC_{50} values of 5.3 ± 0.5 and 24 ± 2 μM, respectively). Five compounds displayed moderate activity against the parasites (IC_{50} = 21−39 μM), whereas the remaining 12 were inactive (IC_{50} > 50 μM). There was no obvious correlation between either the fit score or the conformational energy and the activity of the compounds. A mononitro analogue of **46**

Table 2. Structures of the Test Set Compounds with Their Experimental and CATALYST-Estimated IC_{50} Values against *L. donovani* Axenic Amastigotes or Promastigotes[a]

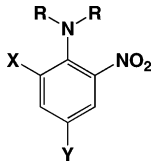

Compound	R	X	Y	Experimental IC_{50} (μM)	Estimated IC_{50} (μM)
15	n-propyl	NO_2	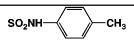	32 ± 13[b]	11
16	n-propyl	NO_2	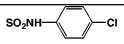	13 ± 3[b]	6.5
17	n-propyl	NO_2	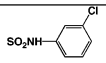	5.5 ± 0.1[b]	2.4
18	n-propyl	NO_2	$SO_2N((CH_2)_3CH_3)_2$	48 ± 7[b]	52
19	n-propyl	NO_2	$SO_2NH(CH_2)_4CH_3$	43 ± 11[b]	50
20	n-propyl	NO_2	$SO_2NH(CH_2)_5CH_3$	26 ± 5[b]	47
21	n-propyl	NO_2		47 ± 4[b]	65
22	n-propyl	H		43 ± 3[b]	43
23	n-butyl	NO_2		5.7 ± 0.1	4
24	H, n-propyl	NO_2	SO_2NH_2	67 ± 18[d]	66
25	n-ethyl	NO_2	SO_2NH_2	69 ± 23[d]	130
26	n-butyl	NO_2	SO_2NH_2	20 ± 0[c]	58
27	n-propyl	H	SO_2NH_2	90 ± 15[d]	61
28	n-propyl	NO_2	$CONH_2$	76 ± 20[d]	57

[a] The error is reported as the standard deviation from the mean of three separate experiments. [b] From ref 10. [b] From ref 8. [d] From ref 8, values against promastigotes.

(compound **57**) was commercially available and was also tested for in vitro antileishmanial activity. This compound was much less active than **46** (IC_{50} value = 98 ± 7 μM).

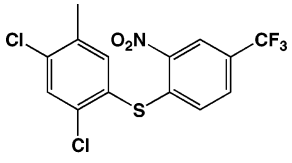

57

Antimitotic and Antitubulin Activity. Compounds **1** and **11** were previously demonstrated to display antimitotic activity by inhibiting leishmanial tubulin assembly. Because the database search was based on a pharmacophore of the dinitroaniline sulfonamides, the compounds identified from this search were expected to have a similar mechanism of action. Surprisingly, unlike compounds **1** and **11**, the seven active compounds identified in this study did not possess antimitotic activity; the cells were not blocked at the G_2/M phases of the cell cycle as observed by flow cytometry (a representative experiment with **46** is shown in Figure 3). Furthermore, compound **46** did not inhibit the assembly of isolated *Leishmania* tubulin as seen with **1** and **11** (Figure 4).

Transmission Electron Microscopy. To provide clues regarding the mechanism of action of the most active compound **46**, morphological changes in *L. donovani* promastigotes were observed by transmission electron microscopy after treatment with this agent. Overall sizes between the control and compound-treated parasites were similar (Figure 5). No disintegrating cells were observed in the control samples, whereas there were several in the compound-treated cells. Most notably, however, mitochondrial dilation was seen in most of the compound-treated cells but only rarely in controls. The area of low electron density around the kinetoplast varied widely from parasite to parasite, ranging from a few hundred nanometers to 2 or 3 μm across. The number of such aberrant cells increased as the concentration of **46** was raised from 1 to 4 μM (not shown). Additionally, granular vacuoles were observed in the compound-treated parasites that may correspond to sections of the large mitochondrion[11−13] observed as a result of the sectioning process.

Table 3. Structures of the Nine Compounds outside of the Training Sets and Test Sets that Were Poorly Predicted by the Pharmacophore with Their Experimental and CATALYST-Estimated IC_{50} Values against *L. donovani* Axenic Amastigotes[a]

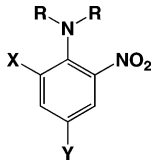

Compound	R	X	Y	Experimental IC_{50} (μM)	Estimated IC_{50} (μM)
29	n-propyl	NO_2	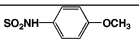	32 ± 15[b]	5.3
30	n-propyl	NO_2	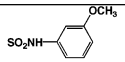	8.1 ± 3.3[b]	2.1
31	n-propyl	NO_2	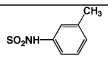	23 ± 1[b]	1.9
32	n-propyl	NO_2	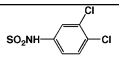	5.0 ± 0.8[b]	1.2
33	n-propyl	NO_2		2.5 ± 0.4	19
34	n-propyl	NO_2	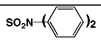	>100[b]	5.6
35	n-ethyl	NO_2		11 ± 3[b]	55
36	n-pentyl	NO_2	SO_2NH_2	9.0 ± 0.7[c]	56
37	n-hexyl	NO_2	SO_2NH_2	12 ± 1[c]	53

[a] The error is reported as the standard deviation from the mean of three separate experiments. [b] From ref 10. [c] From ref 8.

Mitochondrial Fluorescence Assays. To further characterize the mitochondrial morphology, the mitochondrion-specific dye MitoTracker Red 580 was used to stain compound-treated cells. MitoTracker Red 580 selectively stained a large connected mass that spanned the entire parasite (Figure 6). This mass is purported to be the mitochondrion.[11−13] However, parasites treated with **46** displayed punctate staining inside the cell, which may correspond to disjoined mitochondria. The incidence and severity of abnormal morphology increased with higher concentrations of **46**. Also, a large amount of cellular debris was observed in parasites treated with **46** (not shown). Interestingly, treatment with increasing concentrations of compound **46** resulted in decreasing fluorescence of the mitochondrion-specific dye MitoTracker Green FM compared to that of the control as assessed by flow cytometry (Figure 7a). This decrease in fluorescence was similar to that observed after pretreating the parasites with the mitochondrial uncoupler FCCP for 2 h prior to MitoTracker Green FM staining (Figure 7b).

Passive Cell Death Assays. In other reports, mitochondrial effects similar to those observed in this study have been correlated with apoptosis-like, passive cell death (PCD) in the parasites.[14,15] Therefore, two apoptosis assays were performed to determine if compound **46** also induced parasite PCD. The annexin V assay is a determinant of early PCD by measuring the amount of phosphatidylserine exposed on the plasma membrane. Amphotericin B was chosen as a positive control because of its reported ability to cause PCD in *Leishmania*.[16] Propidium iodide (without a cell permeant) was used to assess necrotic parasites with compromised plasma membrane integrity. Flow cytometry showed a few apoptotic parasites in the controls from 24 to 72 h (Figure 8a, only the 72 h results are shown), but a dramatic increase was observed in the number of apoptotic cells in amphotericin B-treated parasites (Figure 8c). Conversely, in parasites treated with **46**, there was a slight increase in annexin V-positive cells from 24 to 72 h compared to the dramatic increase in necrotic cells (Figure 8b). The terminal deoxynucleotidyl transferase (TdT)-mediated dUTP nick end-labeling (TUNEL) apoptosis assay was also performed to analyze end-stage apoptosis via DNA fragmentation. Whereas there were few TUNEL-positive parasites observed in the control sample at 72 h (Figure 9a), a substantial increase in TUNEL-positive parasites after amphotericin B treatment at 72 h was observed (Figure 9c). However, the parasites treated with **46** showed a very modest increase in TUNEL-positive cells (Figure 9b). Taken together, the annexin V and TUNEL assays indicate that compound **46** does not cause significant PCD in the parasites but suggests that necrosis is the primary pathway for cell death.

Infected Macrophage and in Vivo Assays. Compound **46** was able to clear *L. mexicana* parasites from infected J774 murine macrophages (Table 5), reducing the infection in a concentration-dependent manner. Compound **46** is, therefore, active against parasites in host cells in vitro. However, the parasite load in BALB/c mice infected with *L. donovani* was not decreased compared to that in the controls when infected animals were treated with **46** at 50 mg/kg/day for 5 days i.p. (Table 6), showing that **46** is inactive against murine visceral leishmaniasis in vivo, under these treatment conditions.

Discussion

Two highly active antileishmanial compounds, **46** and **48**, and five moderately active compounds were identified by generating a pharmacophore of the antileishmanial activity of dinitroaniline sulfonamides followed by database searching.

Table 4. Structures of the Maybridge Organics Compounds Tested against *L. donovani* Axenic Amastigotes with Their Fit Scores and Conformational Energy Requirements for Mapping onto the Pharmacophore Model[a]

Compound	Structure	Fit Score	Conf. Energy (kcal/mol)	IC_{50} (μM)
38 AW 00911[b]	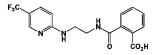	7.1	5.1	>100
39 BTB 01959[c]	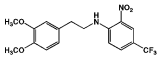	7.1	9.7	>100
40 BTB 09855[c]	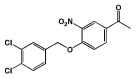	6.9	5.7	>100
41 AW 00835[b]	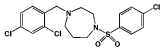	6.8	8.9	72 ± 22
42 AW 01040[b]	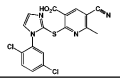	6.6	1.2	21 ± 7
43 AW 00430[b]	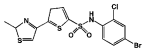	6.6	4.0	66 ± 23
44 AW 00253[b]	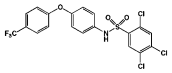	6.6	10.9	25 ± 7
45 AW 00495[b]	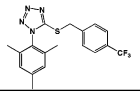	6.6	11.7	32 ± 9
46 BTB 06237[c]	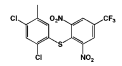	6.5	0.0	0.5 ± 0.2
47 BTB 02382[c]	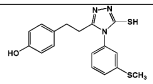	6.4	2.7	>100
48 BTB 06256[c]	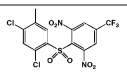	6.4	5.1	2.3 ± 0.8
49 BTB 09564[c]	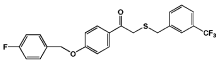	6.4	8.8	>100
50 BTB 06312[c]	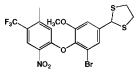	6.3	4.0	>100
51 BTB 04844[c]	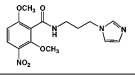	6.3	9.9	>100
52 BTB 02141[c]	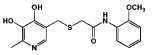	6.2	0.1	>100
53 BTB 03920[c]	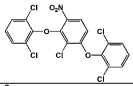	6.2	0.1	80 ± 16
54 AW 00264[b,c]	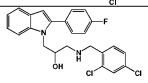	6.1	9.0	37 ± 1
55 BTB 06377[c]	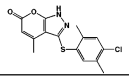	6.0	1.2	39 ± 8
56 BTB 08406[c]	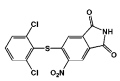	6.0	7.9	60 ± 4

[a] The error is reported as the standard deviation from the mean of three separate experiments. [b] The compounds identified in the pharmacophore-only search. [c] The compounds identified in the pharmacophore-plus-compound **11** search.

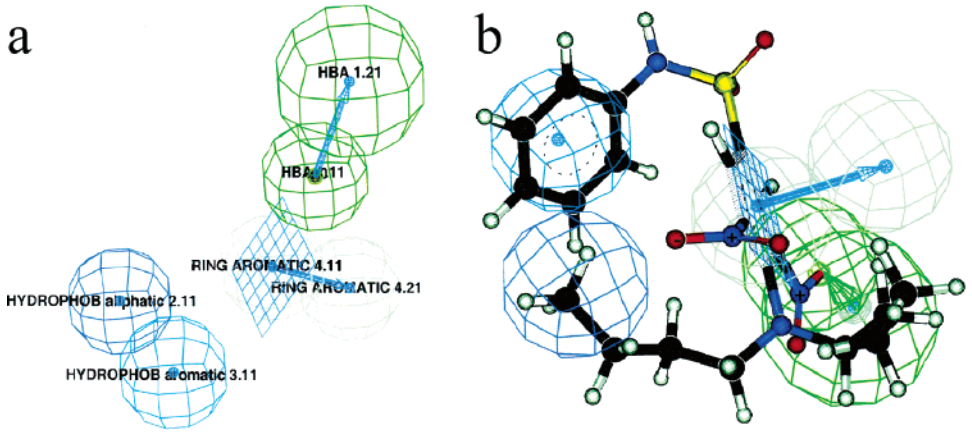

Figure 1. (a) Pharmacophore generated using CATALYST methodology that describes the antileishmanial activity of the dinitroaniline sulfonamides. (b) Compound **11** mapped onto the pharmacophore (different perspective).

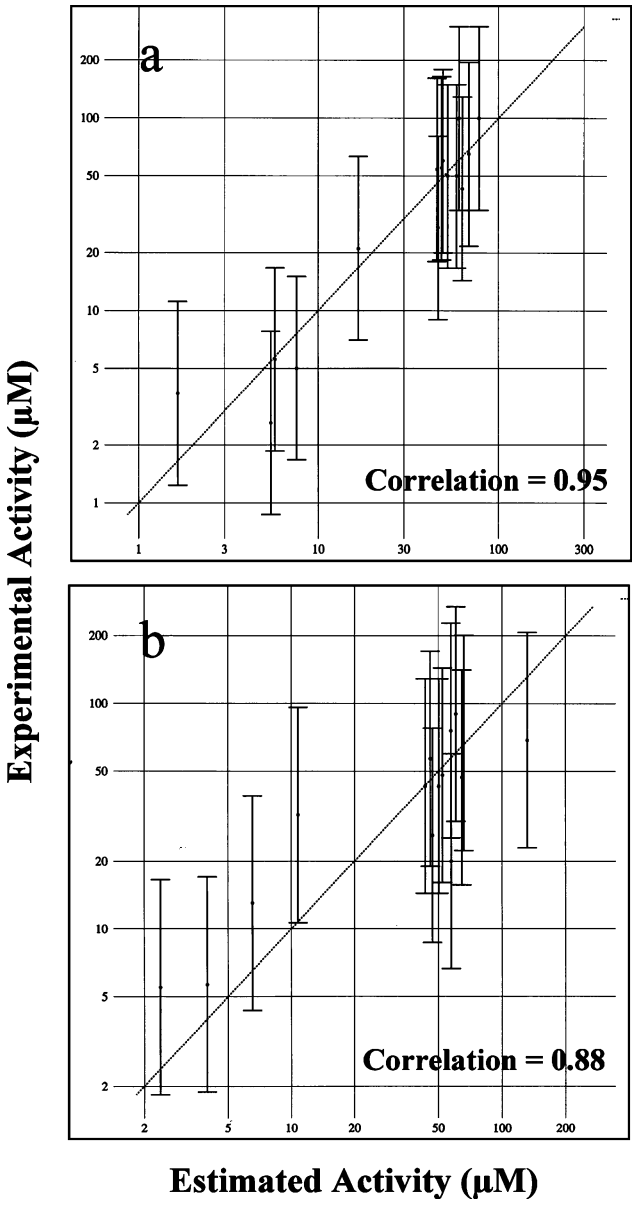

Figure 2. Correlations between the experimental and CATALYST-estimated IC_{50} values of the (a) training set and the (b) test set.

Although the pharmacophore was not statistically robust, it performed well in predicting the activities of 29 out of 38 dinitroaniline sulfonamides. It also yielded several active antileishmanial compounds. Seven of the 19 compounds investigated possessed activity in the axenic amastigote assay at concentrations less than 50 μM, and two were comparable or superior in activity to the lead dinitroaniline sulfonamides **1** and **11**. This success rate is similar to that in other studies with pharmacophore database searches in which the pharmacophores were statistically stronger.[17−20]

The nine compounds for which the pharmacophore was not able to predict activities (Table 3) can be explained by the fact that the functional groups in the pharmacophore lacked specificity. That is, the pharmacophore described the need for an aromatic functionality, but important substitution patterns on the ring were not specified. For example, **29**−**32** all appropriately possess N^1 aromatic rings (position Y), but it was previously observed that groups bulkier than a hydrogen, fluorine, or chlorine atom in the meta or para positions negatively affected their antiparasitic activity.[10] The pharmacophore predicted these compounds to be very active because of the presence of N^1 aromatic rings but did not account for the problematic substitutions at the meta and para positions. Compound **32** was estimated and experimentally shown to be active ($IC_{50} \leq 5$ μM), but the experimental IC_{50} value is approximately four times greater than the estimated IC_{50} value, a difference greater than the allowable error in CATALYST (3-fold difference). Curiously, **33** was predicted to be moderately active but was experimentally found to be highly active. A more rigorously estimated activity (using the best-fit estimation vs the fast fit as reported) predicted the IC_{50} value to be 1.3 μM, bringing **33** in accord with the experimental value (2.5 μM). The fast-fit activity estimation was used to quickly estimate the activities of the compounds in a timely, practical manner. Best-fit estimations, which are highly time consuming to perform, were only used to examine the compounds whose activities were poorly predicted by the pharmacophore. The N^1 bis-aryl compound **34** was predicted to possess activity but was inactive in vitro. As with **29**−**32**, this is likely due to the failure of the pharmacophore to recognize the importance of steric constraints at the N^1 position. For **35**−**37**, these compounds were predicted to be inactive ($IC_{50} \geq 53$ μM) but were experimentally found to be active ($IC_{50} = 9-12$ μM). These compounds had a poor fit into the pharmacophore because of the shorter alkyl chain on the aniline nitrogen (**35**) or the lack of sulfonamide aromatic rings (**36**, **37**). CATALYST considered each feature on the pharmacophore to be equally important to the compounds' activities. However, the activity of **35** suggests that the presence of a three- or four-carbon alkyl chain at N^4 is not as important to activity as the other features. A similar explanation may be

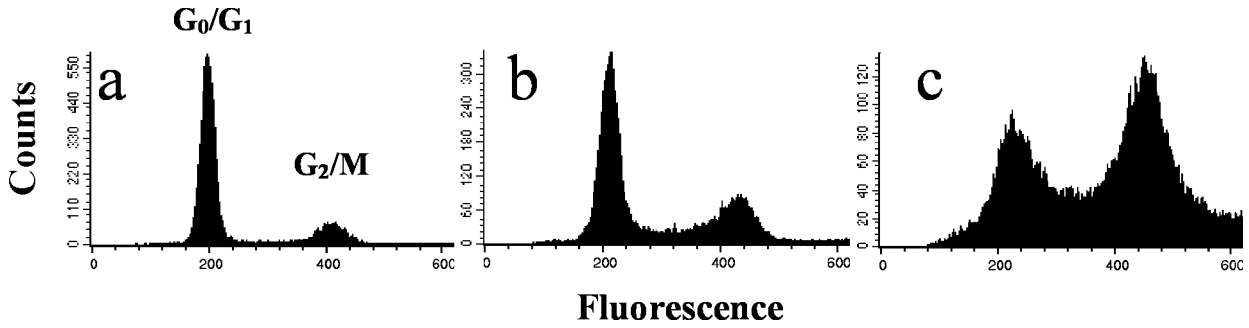

Figure 3. Flow cytometry cell cycle analysis of *L. donovani* promastigotes treated with (a) 1% DMSO, (b) 2 μM compound **46**, or (c) 5 μM compound **1** for 2 days. The histograms shown are representative of three separate experiments.

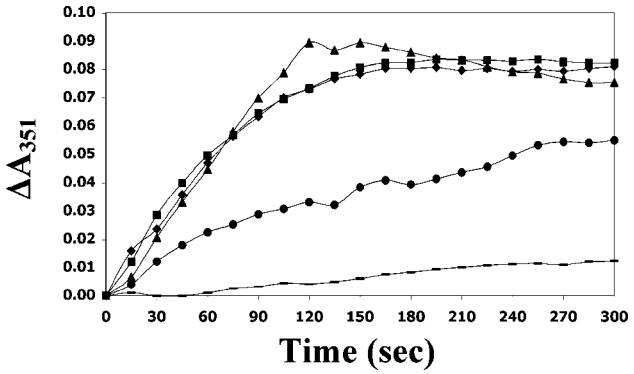

Figure 4. *L. tarentolae* tubulin assembly in the presence of (■) 1% DMSO, (●) 5 μM compound **1**, (-) 10 μM **1**, (◆) 2 μM **46** or (▲) 20 μM **46**. Data shown are representative of three independent experiments.

applied to the activities of **36** and **37**. The added hydrophobicity of their longer alkyl chains may have also contributed to the activity of these compounds.

Unlike the most active dinitroaniline sulfonamides **1** and **11**, the active compounds identified through this database search did not show antimitotic activity and displayed no inhibition of tubulin assembly. A possible explanation for this surprising result is that the pharmacophore that was generated was based on the leishmanicidal activity of the dinitroaniline sulfonamides rather than their antitubulin activity. Pharmacophore generation is more accurate when a wide range of activities is available in the training and test sets. Therefore, we chose to use antileishmanial activities rather than antitubulin activities for pharmacophore generation because the antiparasitic activities had a range of 2 orders of magnitude, whereas the solubility issues limited our range of antitubulin activities to less than 1 order of magnitude.[10] Because of this, the compounds identified in the search may have been more likely to display general antileishmanial activity than specific antitubulin activity. We have previously indicated that mechanisms of action other than microtubule disruption may contribute to the leishmanicidal effect of some dinitroaniline sulfonamide compounds.[9,10] Although compound **1**, an analogue of the original lead compound oryzalin, showed striking antimitotic effects in *Leishmania* at concentrations that blocked parasite growth, oryzalin itself displayed weak antimitotic activity at its IC_{50} concentration.[9] This suggests that an additional mechanism of action is responsible for the antiparasitic activity of this agent. In addition, an investigation of oryzalin for its anticancer potential revealed that this compound inhibits calcium signaling in mammalian cells.[21] Given the lack of antimitotic activity of **46** and these earlier observations, it is likely that the compounds identified in this molecular modeling study display their antileishmanial effects through alternative mechanisms of action. It is also interesting to note that both nitro groups are necessary for the

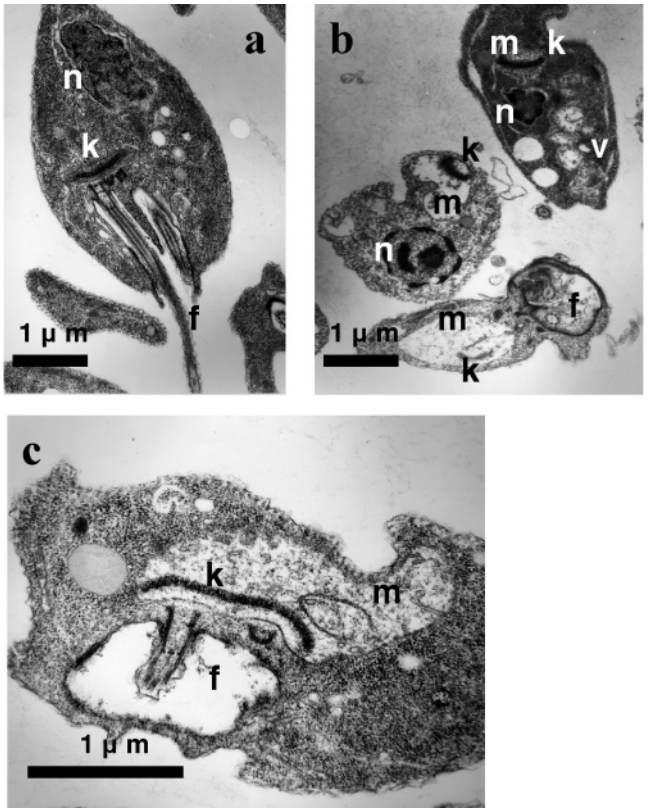

Figure 5. Transmission electron micrographs of *L. donovani* promastigotes incubated for 24 h with (a) 1% DMSO or (b and c) 2 μM **46**. The ultrastructural morphology was observed by transmission electron microscopy. Magnification of a and b is 32 500× and c is is 55 000×. Key: nuclei = n, mitochondria = m, kinetoplasts = k, vacuoles = v, and flagella/flagellar pockets = f.

activity of this compound against *L. donovani* axenic amastigotes because **57**, the mononitro analogue of **46**, is inactive against these parasites.

The most active compound identified in the search (**46**) caused the dilation of the mitochondrion. Similar effects were seen in other studies after applying stress to protozoan parasites of related species. For example, Havens et al. observed "vacuole[s] contain[ing] what remains of the kinetoplast" after treating *L. donovani* with taxol.[22] Mitochondrial swelling and vacuolation was seen in *L. major* in the presence of nitric oxide.[15] In *L. major* treated with staurosporine, dilated mitochondria were also observed.[14] Pentamidine caused the dilation of the mitochondrion in *L. tropica* and *L. amazonensis*.[23,24] Finally, in the related kinetoplastid parasite *Trypanosoma cruzi*, *Bothrops jararaca* snake venom caused "intense swelling of the mitochondrion".[25] Because these effects have been observed in several studies using a wide variety of stress- or death-inducing

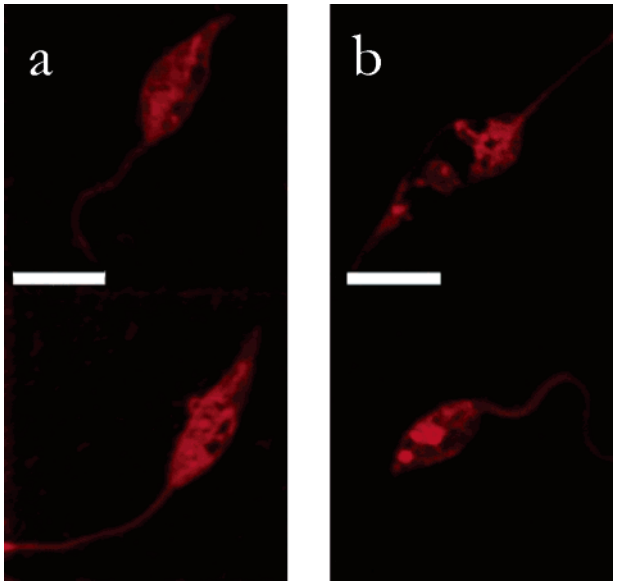

Figure 6. Confocal fluorescence microscopy images of *L. donovani* promastigotes treated with (a) vehicle (1% DMSO) or (b) 4 μM compound **46** for 24 h, followed by staining with MitoTracker Red 580 for 3−5 h. The mitochondrial morphology was observed by confocal microscopy. The bars represent 5 μm.

compounds, the enlargement of the mitochondrion appears to be a common end response of kinetoplastid parasites to drug treatment. However, this response is not necessarily universal. Whereas some compounds cause other significant ultrastructural modifications to the parasites, their mitochondria appear to remain intact. Examples include ketoconazole and formycin B against *L. tropica*,[23] ansamitocin P3 and hemiasterlin against *L. donovani*,[22] and dalrubone[26] or dalrubone analogues against *L. donovani* (unpublished data). Thus, we are unsure whether mitochondrial disruption is the direct mechanism of parasite death after treatment with **46** (as is likely to be the case with pentamidine and other diamidine drugs)[27] or whether upstream targets result in kinetoplast dilation further downstream, leading to parasite death. Furthermore, MitoTracker Red 580 staining of the mitochondrion suggested the fragmentation of the mitochondrion versus the large connected mass as seen in the controls. The ability of the MitoTracker dyes to accumulate in the mitochondrion after the treatment with **46** was reduced, as seen by a decrease in the intensity of fluorescence after MitoTracker Green FM staining. This was parallel to what was observed when the parasites were treated with the uncoupler FCCP. It is, therefore, possible that **46** causes the disruption of the mitochondrial membrane potential. However, it appears unlikely that **46** acts as an uncoupler because it lacks a dissociable proton. Because this compound is expected to be neutral at physiological pH, it is also improbable that mitochondrial accumulation of **46** occurs as observed in *Leishmania* with dications such as pentamidine.[28,29] The reduced accumulation of MitoTracker Green FM may be a function of the reduced mass of this organelle as a result of the treatment with **46**. (MitoTracker Green FM is widely used to estimate mitochon-

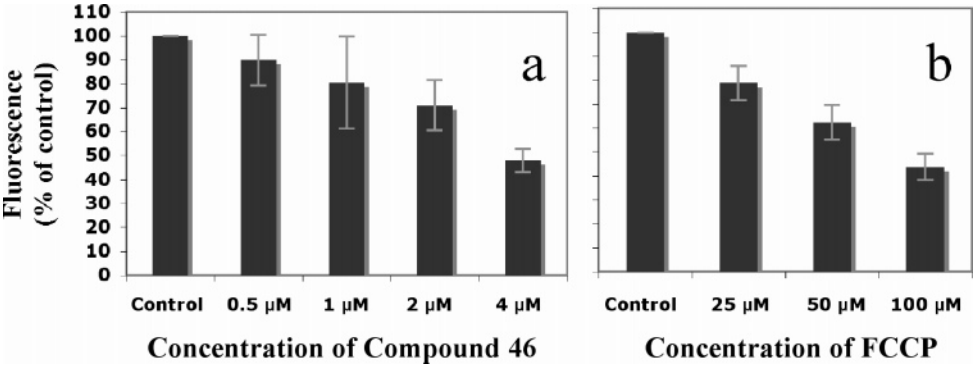

Figure 7. Fluorescence intensity of *L. donovani* promastigotes pretreated with (a) compound **46** for 24 h or (b) FCCP for 2 h and then MitoTracker Green FM for 4 h. The fluorescence intensity was determined by flow cytometry (mean channel fluorescence) and is reported as a percentage of the fluorescence of control parasites. The error bars represent the standard deviation in three separate experiments.

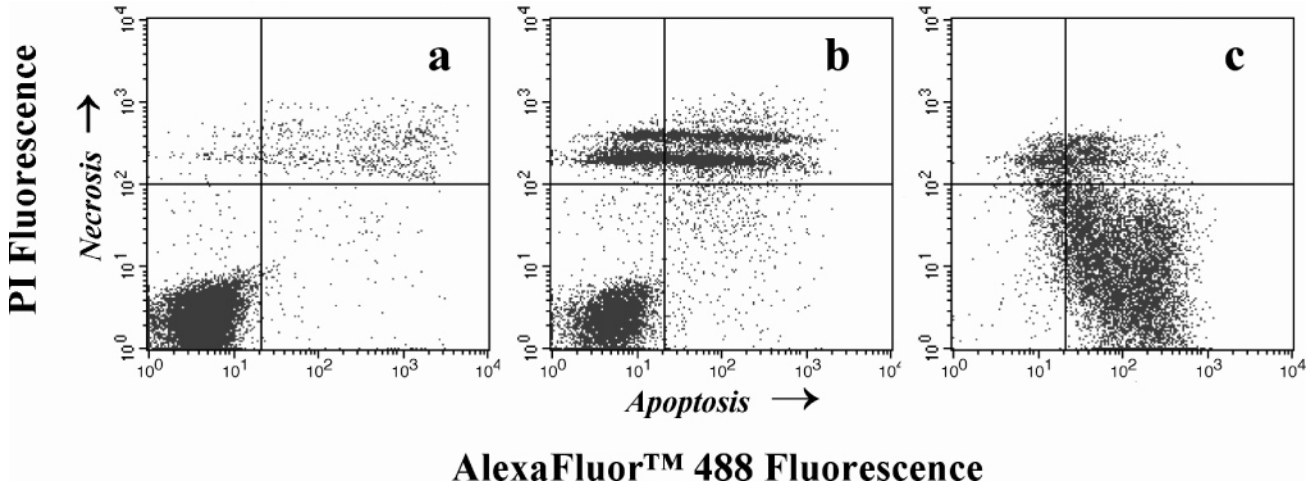

Figure 8. Annexin V assay wherein *L. donovani* promastigotes were treated with (a) the vehicle (1% DMSO), (b) 4 μM compound **46**, or (c) 1 μM amphotericin B for 72 h and then labeled with AlexaFluor 488-conjugated annexin V and propidium iodide. The parasites were analyzed for fluorescence by flow cytometry. The scatter plots shown are representative of two separate experiments.

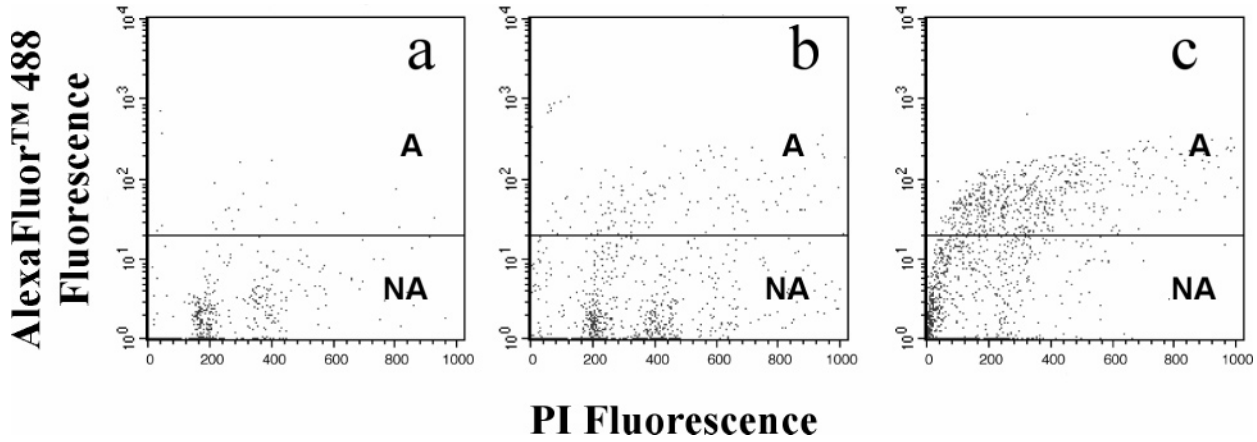

Figure 9. TUNEL assay wherein *L. donovani* promastigotes were treated with (a) the vehicle (1% DMSO), (b) 4 μM compound **46**, or (c) 1 μM amphotericin B for 72 h, labeled with BrdUTP, and then treated with an AlexaFluor 488-conjugated anti-BrdUTP antibody and propidium iodide. The parasites were analyzed for fluorescence by flow cytometry. The scatter plots are representative of two separate experiments. Key: apoptotic = A, nonapoptotic = NA.

Table 5. Percent Reduction of Infection of J774 Murine Macrophages Infected with *L. mexicana*, Relative to that of Controls, after Treatment with Compound **46** or Amphotericin B for 72 h[a]

sample	% reduction in infection
compd **46**, 2 μM	13 ± 0
compd **46**, 4 μM	43 ± 23
compd **46**, 8 μM	68 ± 45
amphotericin B, 25 nM	44 ± 31
amphotericin B, 50 nM	76 ± 13
amphotericin B, 125 nM	96 ± 2

[a] The results are the average (± range) of two separate experiments.

Table 6. Parasitemia (LDUs) Observed after Treating *L. donovani*-infected BALB/c Mice with Compound **46** or Miltefosine via the i.p. Route[a]

sample	LDUs
control	908 ± 98
compound **46**, 50 mg/kg/day	1583 ± 613
miltefosine, 10 mg/kg/day	369 ± 86

[a] The error reported is the standard deviation from the mean LDUs in five mice.

drial mass.) Heteroaromatic compounds containing nitro groups have been shown to cause mitochondrial dilation in *T. cruzi*,[30,31] presumably through the induction of oxidative stress. It is possible, therefore, that **46** exerts its leishmanicidal effects through the formation of reactive oxygen species. However, **46** is more than 4-fold more potent than all the other nitro-containing compounds examined in this study. It is conceivable that the leishmanicidal activity of **46** is due to the specific inhibitory effects on a mitochondrial target protein in the parasite. Further mechanistic studies are required to address this intriguing possibility.

Although many of the aforementioned studies citing the mitochondrial dysfunction also correlate these effects with apoptosis-like passive cell death (PCD) in the parasites,[14,15] the treatment of *L. donovani* with **46** causes a predominance of necrotic cell death as measured by the annexin V and TUNEL assays. However, apoptotic and necrotic death can both be triggered by disruptions in mitochondrial function with the equilibrium between these two forms of death being determined by factors within the cell.[32] Our results with **46** and amphotericin B presented in Figures 8 and 9 are consistent with this hypothesis, with a greater degree of necrosis observed in parasites exposed to the former and a larger portion of PCD seen when the parasites were treated with the latter.

Compound **46** was effective at reducing parasite burdens in vitro in J774 macrophages infected with *L. mexicana*. Unfortunately, **46** appears to be inactive in vivo because it did not reduce the parasite load in *L. donovani*-infected BALB/c mice dosed i.p. with 5 × 50 mg/kg/day of the compound compared to controls. The lack of in vivo activity of **46** may be due to host metabolism or the pharmacokinetic considerations for this compound.

Conclusions

The reported method of pharmacophore development and database searching yielded several active molecules against *Leishmania* and a strong lead compound for further evaluation. Although the compounds did not possess the expected mechanism of action, **46** is potently leishmanicidal in vitro and affects the integrity of the parasite mitochondrion. Further studies into the mechanism of action, structure−activity relationship, and metabolic/pharmacokinetic profile of compound **46** are in progress.

Materials and Methods

Molecular Modeling. Pharmacophore Generation. Synthesis of all dinitroaniline sulfonamide analogues except **12** and **23** (structures in Tables 1 and 2, respectively) was described previously.[8,10] Compounds **12** and **23** were similarly prepared; complete characterizations for these molecules will be described in an upcoming article. The 3D pharmacophore development was carried out using CATALYST 4.7 software (Accelrys, Inc., San Diego, CA). The structures of several dinitroaniline sulfonamide compounds were built from fragments in CATALYST. A CHARMM-like force field as pre-set in the CATALYST program was utilized to ascertain the energy-minimized conformations for each structure. Up to 300 conformational models per compound were generated. The energy cost for each conformer was set to be no more than 20 kcal/mol from the global minimum. The conformational models allowed for molecular flexibility because each conformer was considered in subsequent generation and verification of the pharmacophore. Fifteen diverse compounds were then chosen as the training set representing a range of antileishmanial activities and a

variety of functional groups on the dinitroaniline sulfonamide nucleus. These compounds (including their conformational models) were used to generate the pharmacophore.

From the structures of the training set compounds and their experimentally determined in vitro antileishmanial activities against *L. donovani* axenic amastigotes, the HypoGen algorithm and the default parameters in the AutoGen function in CATALYST were used to generate 3D pharmacophores (called hypotheses in the program). In this methodology, the structure and activity correlations in the training set were rigorously examined. The algorithm found features that were common to the active compounds but excluded from the inactive compounds within conformationally allowable regions of space. Various combinations of five of the following molecular features were used in each round of hypothesis generation: generalized hydrophobic, aliphatic hydrophobic, aromatic hydrophobic, aromatic, hydrogen bond donor, hydrogen bond acceptor, and positive ionizable groups. Six different iterations of the algorithm were performed, and a set of 10 hypotheses was reported for each iteration.

Verifying the Pharmacophore. To determine the validity of each pharmacophore and select the best representation of the structure−activity relationship, the hypotheses were examined for their ability to estimate the activity of both the training set and the test set compounds. The training set consisted of 15 diverse dinitroaniline sulfonamides, whereas the test set was made up of 14 of these compounds. For a valid pharmacophore, a good correlation must be observed between the estimated and experimental activities (with an allowable error of between one-third and three times the experimental activity) for both the training and test sets. To estimate the activity of each compound, the conformation with the lowest root-mean-square (rms) deviation when its atoms were mapped onto the hypothesis was used. HypoGen assumes that all features in the hypothesis have equal weights (contribute equally to the estimated activity) and equal tolerances (each pharmacophore feature must match a corresponding atom on the compound). Both the ability of the best-fitting conformer to match with each feature in the pharmacophore and the conformational energy requirement for the fit are equally important in estimating the activity of the compound. The validity of the pharmacophores was also assessed in a statistical analysis wherein CATALYST calculated the difference in bit scores between the hypothesis generated by CATALYST and a null (random) hypothesis that was not able to predict the activities of the compounds in the training set. Larger bit scores correspond to a greater probability that the hypothesis has predictive power.

Database Searching. The hypothesis generated was used to search the Maybridge compound database. One search was performed with only the hypothesis, and another was performed with the 3D shape of the most active dinitroaniline sulfonamide (**11**) mapped onto the hypothesis to account for the steric contribution of the compound together with the other pharmacophoric features. The activity predictions were based on the fit score of the compounds to the pharmacophore models and the conformational energy requirements for the fit. Specifically, the catDB program in CATALYST allowed the database molecules to be analyzed as a set of conformers. Those within 20 kcal/mol of the minimized conformation were considered for their fit to the hypothesis. Fit scores and conformational energies were reported for each hit after utilizing the best-fit function. The low-fitting compounds (fit score <4.5) and those with high-energy costs (>15 kcal/mol) were not considered for further analysis. The 19 hits with the best fit to the pharmacophore (7 from the pharmacophore-only and 12 from the steric-pharmacophore searches) that were also available from Maybridge were tested in antileishmanial assays.

Antileishmanial Assays. *L. donovani* axenic amastigotes (WHO designation MHOM/SD/62/1S-CL2$_D$) were adapted from promastigotes and maintained in an amastigote medium at 37 °C.[9] The cells (6×10^4) in a final volume of 60 μL were plated in each of the wells in a 96-well plate, except for the negative controls. The compounds were added to the appropriate wells, and 2-fold dilutions permitted a range of concentrations to be examined for each compound. The cells were incubated at 37 °C for 3 days in a humidified environment with 5% CO_2. Cell proliferation was determined by a colorimetric assay using the tetrazolium dye-based CellTiter reagent (Promega, Madison, WI).[33] Several hours after the addition of 12 μL of dye to each of the wells in the 96-well plate, the absorbance was observed at 490 nm on a SpectraMax Plus 384 spectrophotometer (Molecular Devices, Sunnyvale, CA). The IC_{50} values were calculated using the SoftMax Pro software (Amersham Biosciences, Piscataway, NJ) using the dose−response equation $y = [(a - d)/(1 + (x/c)^b)] + d$, where x is the drug concentration, y is the Abs_{490}, a is the upper asymptote of a four-parameter curve, b is the slope, c is the IC_{50} value, and d is the lower asymptote. Each compound was tested in three or more separate experiments.

Vero Cell Toxicity Assay. Vero cells (ATCC, Rockville, MD) were maintained in a minimum essential medium, alpha modification containing Glutamax-I (Invitrogen, Carlsbad, CA), and supplemented with 10% heat-inactivated fetal bovine serum (HI-FBS), 50 units/mL of penicillin, and 50 μg/mL of streptomycin. The cells were treated with the test compounds in a manner similar to that used in the axenic amastigote assay above, except that 1×10^3 cells in a final volume of 100 μL were plated in each of the wells of a 96-well plate.

Cell Cycle Analysis by Flow Cytometry. *L. donovani* promastigotes were grown in promastigote medium, based on RPMI 1640 medium supplemented with 0.2 mM glutamine, 0.1 mM adenosine, 1 μg/mL of folate, 50 units/mL of penicillin, 50 μg/mL of streptomycin, 1× RPMI 1640 vitamins, and 10% HI-FBS. The cells (5×10^6 cells/mL) were incubated with the test compounds or the vehicle (1% DMSO) at 25 °C for 2 days in a humidified environment and 5% CO_2. The cells were concentrated by centrifugation at 3200*g* and fixed with 70% methanol in PBS for at least 2 h. The parasites were then incubated with 10 μg/mL of propidium iodide, 0.1% Triton-X 100, and 5 μg/mL of RNAseA. The cells were then collected by centrifugation and resuspended in PBS to a concentration of 1×10^7 cells/mL. The fluorescence intensity in individual cells was analyzed by flow cytometry using a Becton Dickinson FACSCalibur instrument (Rutherford, NJ).[9]

Tubulin Assembly Assays. Tubulin from *L. tarentolae* was purified as described previously.[9] *L. tarentolae* tubulin (1.5 mg/mL) was incubated in a buffer containing 0.1 mM PIPES (pH 6.9), 1 mM $MgCl_2$, 1 mM EGTA, 10% DMSO, and 1 mM GTP with or without test compounds in deionized water at 30 °C. The tubulin assembly was assessed by monitoring the absorbance (solution turbidity) at 351 nm using a SpectraMax Plus 384 spectrophotometer as described previously.[9]

Transmission Electron Microscopy. *L. donovani* promastigotes were incubated with a compound or vehicle (1% DMSO) for 12−48 h, centrifuged at 3200*g* for 10 min at 4 °C, and then fixed in a 0.1 M phosphate buffer with 4% paraformaldehyde and 0.1 M sucrose for 3 h. The cells were washed four times with a 0.1 M phosphate buffer containing 0.1 M sucrose, then incubated for 1 h in a 1% osmium tetroxide in phosphate buffer, rinsed twice, and set with 2% agarose chilled in an ice bath for 10 min. The agarose was cut into blocks and stained with 2% uranyl acetate and lead citrate.[34] The cells were dehydrated using a 50−100% ethanol gradient, treated with propylene oxide alone, then propylene oxide with Spurr resin (1:1 for 1 h and then 1:2 overnight), and finally embedded in Spurr resin for polymerization overnight. Ultrastructural analysis was performed on a Phillips CM 12 transmission electron microscope (Eidenhoven, The Netherlands).

Detection of Mitochondrial Fluorescence by Microscopy and Flow Cytometry. *L. donovani* promastigotes at 5×10^6 cells/mL were incubated with compound **46** or vehicle (1% DMSO) for 24 h at 25 °C. Up to 1×10^7 cells were collected from each sample and centrifuged at 3200*g* for 10 min at room temperature. The mitochondria were then stained with 100 μM MitoTracker Red 580 (MTR) or MitoTracker Green FM (MTG) (Molecular Probes, Eugene, OR) for 3−5 h at 25 °C on microscope slides pretreated with poly-L-lysine (MTR) or incubated in microcentrifuge tubes (MTG). The parasites were fixed with 3.7% formaldehyde in

promastigote medium for 15 min at 37 °C. For parasites pretreated with carbonyl cyanide 4-(trifluoromethoxy)phenylhydrazone (FCCP), 1×10^7 cells/mL were collected from the cell culture and treated with varying concentrations of FCCP or the vehicle for 2 h. Then, 100 μL of 100 μM MTG was added to each sample and incubated for 3−5 h. The cells were fixed with 440 μL of 8% formaldehyde in medium for 15 min at 37 °C. The cells were centrifuged, resuspended in 1 mL of PBS, and then analyzed by flow cytometry. Microscopic evaluations of MTR-stained cells were performed on a Nikon Eclipse TE300 fluorescence microscope (Tokyo, Japan) and a Zeiss 510 META laser scanning confocal microscope (Thornwood, NY). Flow cytometry on MTG-stained cells was performed as described previously.

TUNEL Assay. *L. donovani* promastigotes (5×10^6 cells/mL) were incubated with compound **46** or the vehicle (1% DMSO) for 48−72 h at 25 °C. An aliquot of 2×10^6 cells was collected by centrifugation at 3200*g* for 15 min at 4 °C and then treated with 1% paraformaldehyde for 15 min followed by 70% ethanol overnight. The TUNEL assay was performed using a kit from Molecular Probes, Inc. as per directions from the manufacturer. Briefly, the DNA was labeled with BrdUTP and an anti-BrdUTP antibody conjugated to AlexaFluor 488. The DNA was also stained with propidium iodide, and then the samples were analyzed by flow cytometry as described above.

Annexin V Assay. *L. donovani* promastigotes (5×10^6 cells/mL) were incubated with compound **46** or the vehicle (1% DMSO) for 24−72 h at 25 °C. An aliquot of 2×10^6 cells was collected by centrifugation at 3200*g* for 15 min at 4 °C. The cells were then rinsed with PBS and resuspended in 100 μL of annexin-binding buffer (100 mM HEPES, 140 mM NaCl, 2.5 mM $CaCl_2$ at pH 7.4), 5 μL of annexin V−AlexaFluor 488 conjugate solution (Molecular Probes, Inc.), and 500 μL of propidium iodide solution (10 μg/mL propidium iodide, 5 μg/mL RNAseA in PBS). After incubation for 30 min at room temperature, 400 μL of the annexin-binding buffer was added to each sample, and an analysis by flow cytometry was performed as described above.

Intracellular Parasite Assay. J774 murine macrophages were maintained in a DMEM medium supplemented with 10% HI-FBS, 2 mM L-glutamine, 50 units/mL of penicillin G, and 50 μg/mL of streptomycin. Then, 1×10^5 J774 macrophages in 200 μL of medium were incubated in each of the wells of a chamber slide overnight at 37 °C, allowing the cells to adhere. The medium was removed, and 200 μL fresh medium containing 1×10^6 *L. mexicana* promastigotes (WHO designation: MNYC/BCZ/62/M379 maintained in promastigote medium as described above) was added to each well. Infection was allowed to occur during incubation at 33 °C overnight. The medium was removed, and the slides were washed several times with Hanks' balanced salt solution. The test compounds or the vehicle (1% DMSO) were prepared in 200 μL of the medium and added to the wells of the chamber slide. The slide was incubated for 3 days at 33 °C, the medium was removed, and the slide was washed several times with phosphate buffered saline (PBS). The cells were fixed with methanol for 30 s, washed with PBS, and stained with 0.05% Giemsa stain for 25 min. The slides were rinsed thoroughly with distilled water.

Antileishmanial Assays in Vivo. The methodology was adapted from a procedure reported by Croft et al.[35] *L. donovani* amastigotes were harvested from the spleen of an infected hamster and suspended in an RPMI 1640 medium at a concentration of 1×10^8 parasites/mL. Twelve week old BALB/c mice were infected with 1×10^7 amastigotes via an injection into the lateral tail vein. Following a seven-day incubation period, the mice were treated with 50 mg/kg/day of compound **46** or 10 mg/kg/day of miltefosine diluted in 200 μL of the vehicle, or the vehicle alone (0.5% w/v methylcellulose, 0.1% v/v Tween-80, 10% DMSO in sterile water), i.p. injected daily for 5 days. Four days posttreatment, the mice were sacrificed and weighed. The livers and spleens were then removed and weighed. Slides were prepared from smears of the liver, fixed for 5−10 s in methanol, and then stained with 0.05% Geimsa stain. The parasite burden in the liver of each animal was reported in Leishman Donovan units (LDUs), defined as the organ mass (g) multiplied by the number of amastigotes per 1000 macrophage nuclei.

Acknowledgment. D.A.D. was supported by a Procter and Gamble graduate fellowship administered through the National Organization of Black Chemists and Chemical Engineers, by a United Negro College Fund/Merck Co. Science Education Initiatives Graduate Fellowship, and by the Military Infectious Disease Research Program of the Department of Defense for a Summer 2004 internship. We also acknowledge NIH Grant AI061021 (to K.A.W.) for financial support. Special thanks are extended to Kathy Wolken at the Campus Microscopy and Imaging Facility and the staff at the Dorothy M. Davis Heart and Lung Research Institute's Flow Cytometry Core Lab, both located at The Ohio State University.

References

(1) Leishmaniasis: Burden of Disease. http://www.who.int/leishmaniasis (posting date Dec 29, 2005).
(2) Magill, A. J. Leishmaniasis. In *Tropical Medicine and Emerging Infectious Diseases*, 8th ed.; Strickland, G. T., Ed.; W. B. Saunders Co.: Philadelphia, PA, 2000; pp 665−687.
(3) Leishmaniasis: Disease Information. http://www.who.int/tdr/diseases/leishmaniasis (posting date Dec 29, 2005).
(4) Singh, S.; Sivakumar, R. Challenges and New Discoveries in the Treatment of Leishmaniasis. *J. Infect. Chemother.* **2004**, *10*, 307−315.
(5) Davis, A. J.; Kedzierski, L. Recent Advances in Antileishmanial Drug Development. *Curr. Opin. Invest. Drugs* **2005**, *6*, 163−169.
(6) Ouellette, M.; Drummelsmith, J.; Papadopoulou, B. Leishmaniasis: Drugs in the Clinic, Resistance and New Developments. *Drug Resist. Updates* **2004**, *7*, 257−266.
(7) Croft, S. L.; Barrett, M.; Urbina, J. Chemotherapy of Trypanosomiases and Leishmaniasis. *Trends Parasitol.* **2005**, *21*, 508−512.
(8) Bhattacharya, G.; Salem, M. M.; Werbovetz, K. A. Antileishmanial Dinitroaniline Sulfonamides with Activity Against Parasite Tubulin. *Bioorg. Med. Chem. Lett.* **2002**, *12*, 2395−2398.
(9) Werbovetz, K. A.; Sackett, D. L.; Delfín, D.; Bhattacharya, G.; Salem, M.; Obrzut, T.; Rattendi, D.; Bacchi, C. Selective Antimicrotubule Activity of *N*1-Phenyl-3,5-dinitro-*N*4,*N*4-di-*n*-propylsulfonilamide (GB-II-5) against Kinetoplastid Parasites. *Mol. Pharmacol.* **2003**, *64*, 1325−1333.
(10) Bhattacharya, G.; Herman, J.; Delfín, D.; Salem, M. M.; Barszcz, T.; Mollet, M.; Riccio, G.; Brun, R.; Werbovetz, K. A. Synthesis and Antitubulin Activity of N^1- and N^4-Substituted 3,5-Dinitroaniline Sulfanilamides against African Trypanosomes and *Leishmania*. *J. Med. Chem.* **2004**, *47*, 1823−1832.
(11) Paulin, J. J. Conformation of a Single Mitochondrion in the Trypomastigote Stage of *Trypanosoma cruzi*. *J. Parasitol.* **1983**, *69*, 242−244.
(12) Simpson, L.; Kretzer, F. The Mitochondrion in Dividing *Leishmania tarentolae* Cells is Symmetric and Circular and Becomes a Single Asymmetric Tubule in Non-Dividing Cells Due to Division of the Kinetoplast Portion. *Mol. Biochem. Parasitol.* **1997**, *87*, 71−78.
(13) Docampo, R.; De Souza, W.; Miranda, K.; Rohloff, P.; Moreno, S. N. J. Acidocalcisomes−Conserved from Bacteria to Man. *Nat. Rev.-Microbiol.* **2005**, *3*, 251−261.
(14) Arnoult, D.; Akarid, K.; Grodet, A.; Petit, P. X.; Estaquier, J.; Ameisen, J. C. On the Evolution of Programmed Cell Death: Apoptosis of the Unicellular Eukaryote *Leishmania major* Involves Cysteine Proteinase Activation and Mitochondrion Permeabilization. *Cell Death Differ.* **2002**, *9*, 65−81.
(15) Zangger, H.; Mottram, J. C.; Fasel, N. Cell Death in *Leishmania* Induced by Stress and Differentiation: Programmed Cell Death or Necrosis. *Cell Death Differ.* **2002**, *9*, 1126−1139.
(16) Lee, N.; Bertholet, S.; Debrabant, A.; Muller, J.; Duncan, R.; Nakhasi, H. L. Programmed Cell Death in the Unicellular Protozoan Parasite *Leishmania*. *Cell Death Differ.* **2002**, *9*, 53−64.
(17) Bhattacharjee, A. K.; Geyer, J. A.; Woodard, C. L.; Kathcart, A. K.; Nichols, D. A.; Prigge, S. T.; Li, Z.; Mott, B. T.; Waters, N. C. A Three-Dimensional in Silico Pharmacophore Model for Inhibition of *Plasmodium falciparum* Cyclin-Dependent Kinases and Discovery of Different Classes of Novel Pfmrk Specific Inhibitors. *J. Med. Chem.* **2004**, *47*, 5418−5426.
(18) Desai, P. V.; Patny, A.; Sabnis, Y.; Tekwani, B.; Gut, J.; Rosenthal, P.; Srivastava, A.; Avery, M. Identification of Novel Parasitic Cysteine Protease Inhibitors Using Virtual Screening. 1. The ChemBridge Database. *J. Med. Chem.* **2004**, *47*, 6609−6615.

(19) Cherkasov, A.; Shi, Z.; Fallahi, M.; Hammond, G. L. Successful in Silico Discovery of Novel Nonsteroidal Ligands for Human Sex Hormone Binding Globulin. *J. Med. Chem.* **2005**, *48*, 3203−3213.
(20) Guner, O.; Clement, O.; Kurogi, Y. Pharmacophore Modeling and Three-Dimensional Database Searching for Drug Design Using Catalyst: Recent Advances. *Curr. Med. Chem.* **2004**, *11*, 2991−3005.
(21) Powis, G.; Gallegos, A.; Abraham, R. T.; Ashendel, C. L.; Zalkow, L. H.; Dorr, R.; Dvorakova, K.; Salmon, S.; Harrison, S.; Worzalla, J. Inhibition of Intracellular Ca^{2+} Signaling, Cytotoxicity and Antitumor Activity of the Herbicide Oryzalin and Its Analogues. *Cancer Chemother. Pharmacol.* **1997**, *41*, 22−28.
(22) Havens, C. G.; Bryant, N.; Asher, L.; Lamoreaux, L.; Perfetto, S.; Brendle, J. J.; Werbovetz, K. A. Cellular Effects of Leishmanial Tubulin Inhibitors on *L. donovani*. *Mol. Biochem. Parasitol.* **2000**, *110*, 223−236.
(23) Langreth, S. G.; Berman, J. D.; Riordan, G. P.; Lee, L. S. Fine-Structural Alterations in *Leishmania tropica* within Human Macrophages Exposed to Antileisihmanial Drugs in Vitro. *J. Protozool.* **1983**, *30*, 555−561.
(24) Croft, S. L.; Brazil, R. P. Effect of Pentamidine Isethionate on the Ultrastructure and Morphology of *Leishmania mexicana amazonensis in vitro*. *Ann. Trop. Med. Parasitol.* **1982**, *76*, 37−43.
(25) Gonçalves, A. R.; Soares, M. J.; de Souza, W.; DaMatta, R. A.; Alves, E. W. Ultrastructural Alterations and Growth Inhibition of *Trypanosoma cruzi* and *Leishmania major* Induced by *Bothrops jararaca* Venom. *Parasitol. Res.* **2002**, *88*, 598−602.
(26) Salem, M. M, Werbovetz, K. A. Antiprotozoal Compounds from *Psorothamnus polydenius*. *J. Nat. Prod.* **2005**, *68*, 108−111.
(27) Bray, P. G.; Barrett, M. P.; Ward, S. A.; de Koning, H. P. Pentamidine Uptake and Resistance in Pathogenic Protozoa: Past, Present and Future. *Trends Parasitol.* **2003**, *19*, 232−239.
(28) Basselin, M.; Denise, H.; Coombs, G.; Barrett, M. Resistance to Pentamidine in *Leishmania mexicana* involves exclusion of the drug from the mitochondrion. *Antimicrob. Agents Chemother.* **2002**, *46*, 3731−3738.
(29) Mukherjee, A.; Padmanabhan, P.; Sahani, M.; Barrett, M.; Madhubala, R. Roles for Mitochondria in Pentamidine Susceptibility and Resistance in *Leishmania donovani*. *Mol. Biochem. Parasitol.* **2006**, *145*, 1−10.
(30) Muelas-Serrano, S.; Pérez-Serrano, J.; Gómez-Barrio, A.; Arán, V. J.; Rodríguez-Caabeiro, F. Ultrastructural Alterations Induced by Nifurtimox and Another Nitro Derivative on Epimastigotes of *Trypanosoma cruzi*. *Parasitol. Res.* **2002**, *88*, 97−101.
(31) Voigt, W.-H.; Bock, M.; Gönnert, R. Ultrastructural Observations on the Activity of Nifurtimox on the Causative Organism of Chagas' Disease I. *Trypanosoma cruzi* in Tissue Cultures. *Arzneim.-Forsch.* **1972**, *22*, 1586−1589.
(32) Kroemer, G.; Dallaporta, B.; Resche-Rigon, M. The Mitochondrial Death/Life Regulator in Apoptosis and Necrosis. *Annu. Rev. Physiol.* **1998**, *60*, 619−642.
(33) Werbovetz, K. A.; Brendle, J. J.; Sackett, D. L. Purification, Characterization and Drug Susceptibility of Tubulin from *Leishmania*. *Mol. Biochem. Parasitol.* **1999**, *98*, 53−65.
(34) Reynolds, E. S. The Use of Lead Citrate at High pH as an Electron-Opaque Stain in Electron Microscopy. *J. Cell Biol.* **1963**, *17*, 208−212.
(35) Croft, S. L.; Neal, R. A.; Pendergast, W.; Chan, J. H. The Activity of Alkyl Phosphorylcholines and Related Derivatives against *Leishmania donovani*. *Biochem. Pharmacol.* **1987**, *36*, 2633−2636.

JM060156V